Calculated and measured Auger lineshapes in clean Si(100)2×1, SiO$_x$ and Si-NO

Calculated and measured Auger lineshapes in clean Si(100) 2 × 1, SiO$_x$ and Si–NO†

A G B M Sasse‡, H Wormeester, M A van der Hoef and A van Silfhout

University of Twente, Department of Applied Physics, PO Box 217, 7500 AE, Enschede, The Netherlands

Abstract. The measurements were performed on the clean 2 × 1 reconstructed Si(100) surface and this surface exposed to molecular oxygen (O$_2$) or nitric oxide (NO) at room temperature. The data were corrected for electron loss and spectrometer distortions using our newly developed deconvolution method. This method which uses global approximation and spline functions can overcome several difficulties with respect to deconvolution and allows us to derive high-quality Auger lineshapes from the Si L$_{2,3}$VV Auger electron spectra.

Our experimentally obtained Auger lineshapes were compared with theoretical lineshapes utilising quantum chemical cluster calculations. We used this type of calculation for the interpretation of the Auger lineshape in the actual p-like and s-like partial local density of states for different types of silicon atom. The observed intensities of the major features are in reasonable agreement with our calculations.

1. Introduction

Auger electron spectroscopy (AES) is a widely used technique for surface chemical element analysis [1]. Earlier studies [2–12] showed that analysis of the lineshape in the core valence–valence (CVV) Auger spectrum can provide information on the local chemical environment of the target atomic species. However, the measured CVV Auger intensity $N(E)$ is distorted by all kinds of loss such as elastic and inelastic scattering, interaction with collective oscillations (plasmons, etc) and instrumental broadening [13–16]. It is well established that corrections for these Auger line profile distortions [16–19] are of sufficient quality to compare the experimental results with theoretical lineshapes as calculated in [3, 20, 21].

It has been shown that for covalent molecules, e.g. silicon, the inter-atomic Auger matrix elements can be neglected [10, 21–24]. This extreme local behaviour of the Auger process enables us to model the half-infinite Si surface in terms of a finite cluster of silicon atoms. Quantum chemical cluster calculations performed in real space can be utilised to obtain the angular momentum-dependent partial local density of states (PLDOS) of a surface silicon atom and to calculate the CVV Auger lineshape $A(E)$. One

---

of the main advantages of this type of quantum chemical cluster calculation is the possibility of including the influence of surface geometry and chemical bonding.

The aim of this paper is to compare experimental and calculated Auger lineshapes and to interpret them in terms of the actual p-like and s-like PLDOS.

This work is organised as follows. In § 2 we shall discuss the data processing required to obtain the Auger lineshape from the Si $L_{2,3}$VV Auger spectrum. The quantum chemical calculation aspects are explained in § 3. In § 4 we compare the calculated and measured Auger lineshapes. Concluding remarks are given at the end of this paper.

The procedure for surface cleaning, gas handling and Auger measurements can be found in [12, 25, 26].

2. Data processing

If one wants to perform an Auger lineshape analysis, a careful correction for the distortions is necessary which requires a careful study of its nature [15]. The distortions were removed [27] using essentially the same concept as described in [14]. It was assumed in [14] that the lineshape deformation is proportional to the energy distribution $V(E)$ of a reflected beam of electrons with the same energy as the dominant Auger transition. The measured Auger spectrum $dN(E)/dE$ can be deconvoluted by this response function $dV(E)/dE$, thus yielding the true Auger lineshape $A(E)$:

$$dN(E)/dE = A(E) * dV(E)/dE \qquad (1)$$

with * defining the convolution operation.

Our deconvolution method has been discussed extensively elsewhere [12, 15, 28]. The method is based on global approximation using splines [29] and a modified non-linear least-squares fitting (Levenberg–Marquardt) routine [30]. In the global approximation the line regions over the entire spectrum are correlated. This property is used to suppress uncorrelated frequencies, such as noise. An example of this scheme for clean silicon is depicted in figure 1.

3. Cluster calculations

Within the independent-particle approximation and owing to the core hole localisation, it was shown [3] that the Auger lineshape can be expressed in terms of atomic Auger matrix elements and of the atomic angular momentum components of the LDOS localised on the same site as the core hole. If the lineshape does not reflect the final-state hole configuration, which is the case for s–p materials such as silicon [2, 20–24], information on the local density of occupied states can be obtained. We can express, to first order, the Auger lineshape in terms of convolution products of the PLDOS:

$$A(E) = C_{ss}D_s(E)*D_s(E) + C_{sp}D_s(E)*D_p(E) + C_{pp}D_p(E)*D_p(E) \qquad (2)$$

where C_{kl}(l, k $\equiv$ s, p) are the atomic matrix elements and $D_k(E)$ and $D_l(E)$ are the k-like LDOSs at a position of the atom in which the initial hole is produced.

The variation in the two electron Auger matrix elements C_{kl} across the valence band is predominantly due to the number of decaying channels for the Auger electrons (pp, 46; sp, 24; ss, 3) [7], which is governed by the selection rules of the atomic angular momentum of the electrons involved in the Auger process [2–4, 10–12].
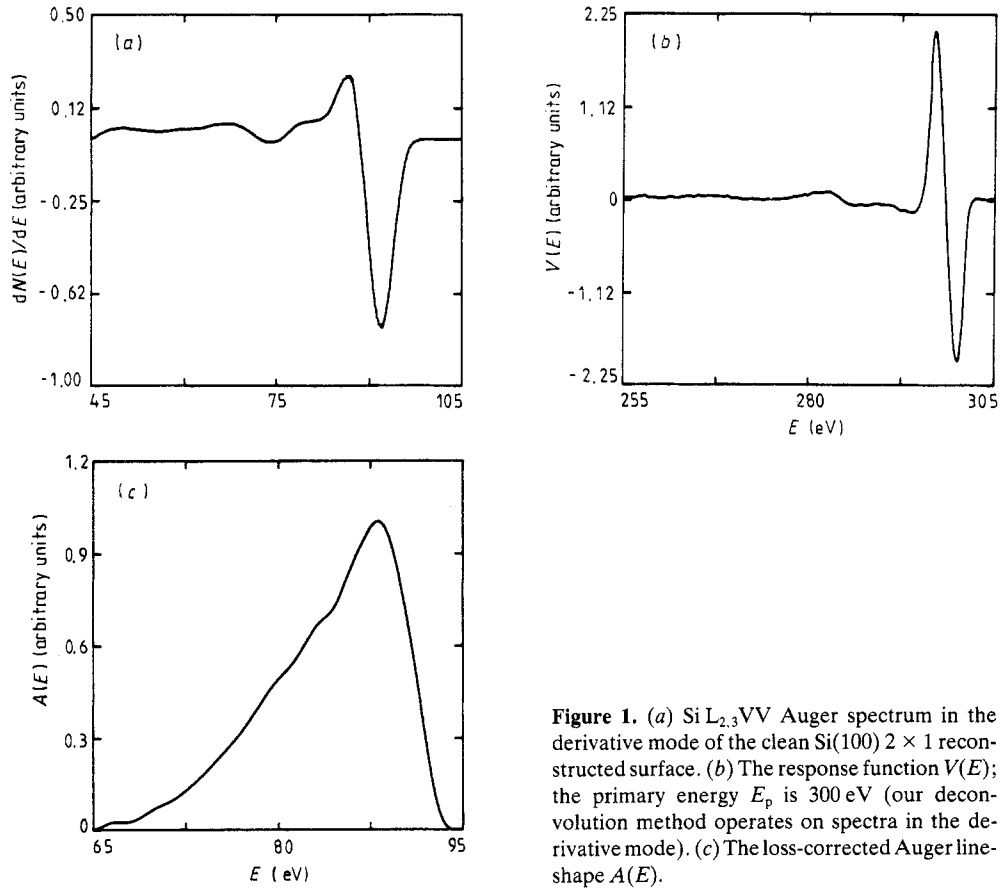
Figure 1. (*a*) Si L$_{2,3}$VV Auger spectrum in the derivative mode of the clean Si(100) 2 × 1 reconstructed surface. (*b*) The response function $V(E)$; the primary energy E_p is 300 eV (our deconvolution method operates on spectra in the derivative mode). (*c*) The loss-corrected Auger lineshape $A(E)$.

**Table 1.** Peak positions of the LDOS of SiO$_x$ (the value in vacuum is 0 eV)

x	Peak energy (eV)					
0	−8.4	−12.6	−16.6	−20.4	−24.6	−28.2
0.5	−9.1	−12.2	−16.0	−21.0	−24.9	—
1	−7.2	−10.5	−15.2	−17.9	−21.9	—
1.5	−9.2	−13.5	−16.8	−20.3	—	—
2	−7.7	−14.1	—	−20.1	—	—

In equation (2) we utilise a theoretical PLDOS $D_{k,l}$ and D_l (tables 1 and 2), obtained from semi-empirical quantum chemical cluster calculations. For our cluster modelling of the Si(100) 2 × 1 substrate and its adsorbates, we have used Si$_9$O$_x$H$_{14}$ (with x = 2, ..., 5) [31], Si$_{20}$H$_{18}$–NO, Si$_{22}$H$_{18}$–NO [26] and Si$_{27}$H$_{24}$ [27] clusters. For the back-bond atoms the ideal bulk geometry of silicon ($d_{Si–Si}$ = 2.35 Å, and tetrahedral angles) has been used, whereas the surface atoms are subject to an asymmetric 2 × 1 reconstruction [32, 33] as used in [34]. We used hydrogen to terminate the silicon substrate, thus obtaining boundary conditions of sufficient quality ($d_{Si–H}$ = 1.41 Å [26]). The details of this type of calculations have been discussed elsewhere [26, 31, 35, 36].

Table 2. Peak positions of the LDOSs for silicon atoms coordinated to the nitrogen atom of the NO molecule for the first-layer dimer and the second-layer dimer (the value in vacuum is 0 eV).

				Peak energy (eV)						
				First-layer dimer						
Up atom	—	−4.0	−9.6	−14.4	—	−19.3	—	−28.6	−30.7[a]	−42.5
Down atom	—	−4.0	−9.4	−14.6	—	−19.4	−25.0	−28.6	−30.7	−42.6
Back bond up	−1.5	—	−8.4	—	−16.9	−20.0	−25.3	—	−31.0	—
Back bond down	—	−4.0	−9.1	—	−18.1	—	−25.5	—	−31.0	—
				Second-layer dimer						
Up atom	—	—	−8.6	−14.8	−17.5	−19.7	−24.2	−28.1	—	−42.6
Down atom	—	—	−9.2	−16.0	−16.8	−19.7	−24.3	−28.1	−30.2	−42.6

[a] Weak features.
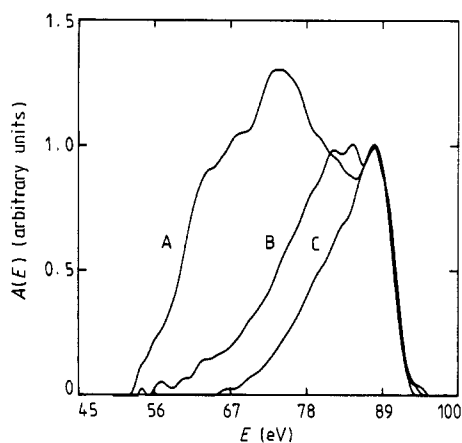
Figure 2. The experimentally obtained Auger lineshapes: curve A, SiO_x; curve B, Si–NO, with NO chemisorbed molecularly; curve C, the clean Si(100) 2 × 1 reconstructed surface.

4. Results and discussion

4.1. Introduction

In figure 2 we show the experimental results of the three interfaces—c-Si(100)–vacuum, c-Si(100)–SiO_x and c-Si(100)–NO with NO adsorbed molecularly [26, 31, 35, 36]. The SiO_x interface consists of a saturated oxide layer with a thickness of the order of a few monolayers chemisorbed at room temperature. The coverage of NO, adsorbed at 300 K on the silicon surface is about 15% of a monolayer [26]. Curves A–C in figure 2 are scaled with respect to elemental silicon. The peak positions in the Auger lineshapes are analysed in the derivative mode $dA(E)/dE$ to enhance the peak positions (see table 3). We have also calculated the differential Auger lineshape applying equation (2). The results are listed in table 3.

To first order, the kinetic energy of the Auger electrons obtained experimentally can be connected to the cluster calculations using [10]

$$E_{kin} = E_{L2,3} - E_{v1} - E_{v2} - E_f \qquad (3)$$

where $E_{L2,3} - E_f$ is approximated by translating the main peak to its average known experimental value (e.g. the value for c-Si(100) is 91.8 eV). E_{v1} and E_{v2} are related to

Table 3. Peak positions of the $dA(E)/dE$ of SiO$_x$ ($x = 0, 0.5, \ldots, 2$) and Si–NO.

x	Peak position (eV)											
				SiO$_x$: calculated								
0	—	—	91.9	86.5	—	82.3	79.0	74.0	71.3	65.6	—	—
0.5	—	—	90.4	—	—	82.7	78.1	—	70.6	66.0	—	61.4
1	—	93.8	90.5	86.5	—	82.3	79.2	75.5	70.8	67.5	64.2	—
1.5	—	—	89.1	—	85.0	82.0	78.0	74.6	70.7	65.6	—	—
2	—	93.6	—	87.0	—	81.1	—	74.9	68.9	—	—	—
				Si–NO, first-layer dimer: calculated								
Dimer up	—	95.5	90.1	—	85.0	—	79.5	74.7	—	68.8	—	62.1
Dimer down	—	94.8	90.2	—	83.6	—	79.5	—	70.9	—	63.1	—
Back bond up	98.4	—	92.0	—	—	81.1	—	74.5	—	68.5	—	—
Back bond down	—	95.2	90.5	—	—	81.1	78.6	73.4	—	68.3	—	—
				Si–NO, second-layer dimer: calculated								
Dimer up	—	96.2	91.4	—	84.2	—	79.8	74.0	71.1	—	—	62.9
Dimer down	—	95.0	90.5	—	83.2	—	—	74.7	69.7	—	—	62.4
				Measured								
Si	—	—	92.0	86.5	—	82.4	78.6	74.0[a]	72.0	66.7	—	—
SiO$_x$	—	93.8	90.3	86.8	—	82.7	79.2	74.1	70.5	65.8	—	60.1
SiO$_x$ [41]	—	—	—	84.5	—	82.0	78.0	75.0	69.0	—	64.0	—
SiO$_2$ [41]	—	—	—	—	—	—	78.0	—	—	66.0	—	61.5
SiO$_x$ [34]	—	—	89.0	85.0	83.0	—	79.0	75.0	71.0	69.0	—	—
SiO$_x$[b]	—	—	90.4	—	83.0	—	—	—	70.0	—	—	62.0
Si–NO	—	93.4	91.4	88.5	85.0	81.6	77.9	73.8	70.5	67.3[a]	64.2[a]	—
Si–NO[c]	97.5	95.0[a]	90.3	87.6	84.2	81.0	77.4	73.6	69.6	67.5[a]	64.8	62.8
Si$_x$N$_y$[d]	97.5	93.6[a]	91.7	—	85.5	81.8	77.0	74.0	70.7[a]	68.2[a]	65.0[a]	62.0

[a] Weak features.
[b] $dN(E)/dE$ LVV spectrum. The peak position is the maximum negative-going peak which induces a small difference with the peaks in the $A(E)$ mode [37–39].
[c] Partial dissociation; exposed to 2000 L NO at 550 K.
[d] Heated to 1050 K after finishing the exposure (2000 L at 300 K).

the peak positions in the LDOS spectra. E_f is the energy loss related to the effective work function of detector and substrate [36].

4.2. Clean Si(100)

The main peak of the spectrum of clean silicon can be unambiguously interpreted as a pp Auger process and the sp contributions are responsible for the structure in the low-energy tail. The ss contributions are negligible in all the spectra depicted (figure 3).

The peaks at about 86.5 and 82.4 eV (table 3) can be associated with the pp Auger process located at the dimer-down atom and its back-bond atom (figures 3(b) and 3(d)). Both features can be related to the dimer reconstruction of the 2 × 1 surface and whether they are sensitive for the kind of surface (super)structure. This is in agreement with differences in fine structure found experimentally at about 81–84 eV [37–39] for Si(100), Si(111) and Si(110). The structure at about 79, 74, 72 and 67 eV is dominated by the sp Auger transitions. Varying the ratio of the number of back-bond atoms to those in the first-layer dimer (figure 4(a)) atoms reveals that these features can be related to bulk contributions in the Auger lineshape.

In figure 4(b) the individual atomic contributions to the Auger lineshape with respect
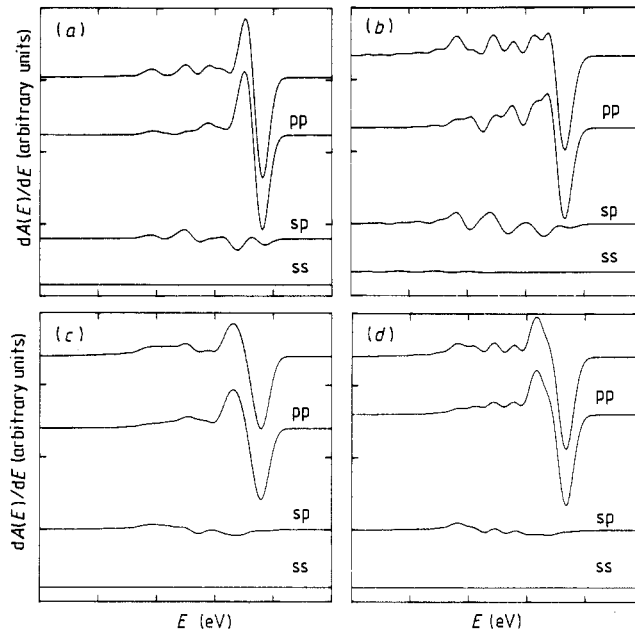
Figure 3. The influence of different types of surface atoms on the Auger spectra: (*a*) dimer up; (*b*) dimer down; (*c*) back bond connected to dimer up; (*d*) back bond connected to dimer down. The width of the kinetic energy axis is 60 eV. The zero of this axis depends on the energy of the core hole and the effective values for the work functions of the surface and the detector.

to the probing depth are summed, weighted by the distribution within a few atom layers at the surface and compared with the actual measurement. We notice good overall agreement with figure 4(*a*), curves D and E, and figure 4(*b*), curve A, with respect to its relative intensity. This ratio of dimer to back-bond atoms of the best fit is in good overall agreement with the expected probing depth (a few atom layers).

Furthermore, additional peak structures can be revealed with respect to the uncorrected $L_{2,3}VV$ Auger spectrum (only peaks at 91.8 and 81 eV can be resolved [12]).

High binding energy levels below -20 eV, revealed by our calculations [27], could not be resolved in the Si $L_{2,3}VV$ spectra, because this part of the spectrum overlaps with the Coster–Kronig Auger transition $(L_1L_{2,3})$ [40]. This could be the reason why the calculation of the Auger matrix elements for $L_1L_{2,3}V$ Auger transitions does not fit well with experimental results [3] and may explain why the lineshape of the $L_1L_{2,3}V$ spectra is broader than one would expect on the basis of x-ray photoelectron spectroscopy measurements of 2s core hole widths [3].

4.3. SiO_x

The initial oxidation of silicon surfaces has been the subject of many investigations ([2, 25] and references therein). The main peaks in the uncorrected $dN(E)/dE$ spectrum are 90.4, 83, 70 and 62 eV (table 3). These structures are also resolved in our calculations and will be compared with previous published results. It can be easily verified, utilising equation (3), that the 82.7 eV transition (tables 1–3 and figure 5) in the $SiO_{1/2,3/2}$ units is predominantly pp like, constituted of valence electrons of p type of approximately -9 eV [31]. In the $SiO_{1,2}$ units the sp transitions are more dominant (about -7 eV
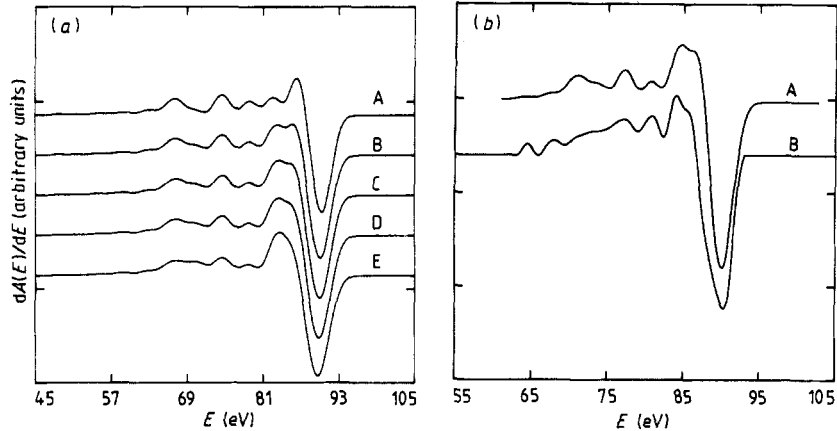
Figure 4. (*a*) Calculated dA/dE as a function of the ratio of the dimer atoms to back-bond atoms: curve A, 1:0; curve B, 1:1; curve C, 1:2; curve D, 1:3; curve E, 0:1. The first numbers in the ratios are the numbers of dimer atoms and the second numbers are the numbers of back-bond atoms involved in the calculation. (*b*) Curve A, calculated d$A(E)$/dE spectrum (ratio 1:2); curve B, loss-corrected experimentally obtained d$A(E)$/dE.

p-like and about -13 eV s-like valence electrons). The pp main transition (about -7 eV) in the SiO$_{1,2}$ units gives rise to features at about 85 eV, which are absent in the SiO$_{1/2,3/2}$ units (see table 3). The pp transition Auger intensity decreases and the ss transition Auger intensity increases at the full oxidation stage (SiO$_2$). The contributions of the ss Auger transitions can therefore not be neglected. In [40], features at about 82 eV were also observed at an early oxidation stage. The character of our calculated Auger transitions for not fully oxidised silicon at about 82.5 eV, which are composed of p-type electrons situated at the top of the valence band, is consistent with the experimental results in [37–39] and supports the assignment of this peak to Si–O bond formation in the first layer.

The Auger transition at about 70 eV is composed of ss- and sp-type contributions and has been attributed to bulk-like oxide [37, 38]. In the calculated SiO$_{1/2}$ spectrum this peak is almost absent and increases upon further oxidation. Furthermore, this peak is shifted towards lower kinetic energy (about 69 eV) at more advanced oxidation stages, a phenomenon which has also been observed experimentally [37, 41]. However, the 70 eV transition also emerges when atomic oxygen is bridge bonded to dimers or back bonds (SiO$_1$ and SiO$_{3/2}$) and can therefore not entirely be attributed to bulk-like oxide (SiO$_2$).

The peak at about 62 eV, which has been assigned to unstable silica [41, 42], is also predominantly an ss-like Auger transition (about -20 eV) in the LDOS. However, this peak emerges in all oxidation stages and even in the LDOS spectrum of the clean silicon surface (figure 2). This peak in the LDOS remains approximately constant for SiO$_x$ ($x = 1, \frac{3}{2}$ and 2). The existence of this peak even in SiO$_2$ suggests that it cannot be attributed entirely to unstable silica. Furthermore, this peak can be composed of contributions from several SiO$_x$ units, which could be the cause for the shift of this peak in the calculated spectra, for several oxidation stages [25, 40–43].

The main peak of the Si L$_{2,3}$VV Auger transition at 91.8 eV for clean Si is shifted to about 90.4 eV upon oxidation. The shift of about 1.4 eV in the Auger spectrum is also observed in the d$A(E)$/dE calculation (table 3, 91.9 eV (SiO$_0$)–90.5 eV (SiO$_1$)).
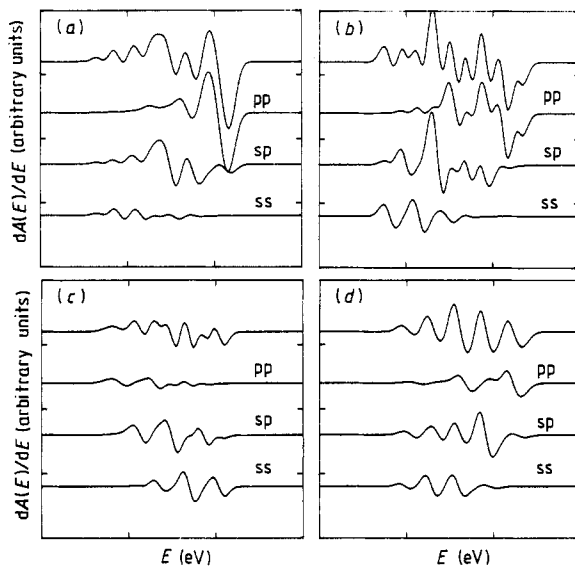
Figure 5. The calculated $\mathrm{d}A(E)/\mathrm{d}E$ spectrum of SiO: $(a)\ x = 0.5$; $(b)\ x = 1$; $(c)\ x = 1.5$; (d) $x = 2$. The width of the kinetic energy axis is 60 eV. The zero of this axis depends on the energy of the core level and the effective value for the work functions of the surface and the detector.

Furthermore, the shift of the main peak is even larger for SiO_2. The shifts in the calculated spectra are completely caused by changes in the energy levels of the valence electrons upon oxygen adsorption. No correction for possible core-level shifts upon variation of the chemical environment, which we believe are negligible, has been made.

Most of the transitions at 93.8, 90.3, 86.8, 82.7, 79.2, 74.1, 70.5 and 65.8 eV of the SiO_x spectrum are resolved by the calculated results of SiO_1: 93.8, 90.5, 86.5, 82.3, 79.2, 75.5, 70.8, 67.5 and 64.2 eV (table 3). This is consistent with the expected dominant SiO_1 phase after an initial oxidation at 300 K.

If we now compare the calculated results with the loss-corrected measured data, most of the additional structures predicted (table 3 and figure 6) are resolved experimentally. We observe that all four stages resemble part of the measured spectrum, which supports the results in [44], where a multiple-bonding configuration was suggested. They found a ratio of SiO_x $(x < 2)$ of approximately 33% each.

The p-type character of the LDOS of the clean Si surface changing upon adsorption to an s-type LDOS makes it impossible to fit completely the whole measured spectrum (figure 6, full curves) with a calculated spectrum (figure 6, dotted curves). In the $SiO_{1/2}$ (mainly p type) we observe quite good agreement at the high-kinetic-energy part (p type) of the spectrum but this is not so for $SiO_{3/2}$ (mainly s type). The best overall agreement is obtained for SiO_1. No significant SiO_2 components were found. The intensities of the calculated spectra are not to scale with respect to each other. This is for convenience in comparing their peak positions, because the relative intensity decreases on further chemisorption.

4.4. Si–NO

From earlier investigations [26] we have argued that the NO molecule is bonded as a
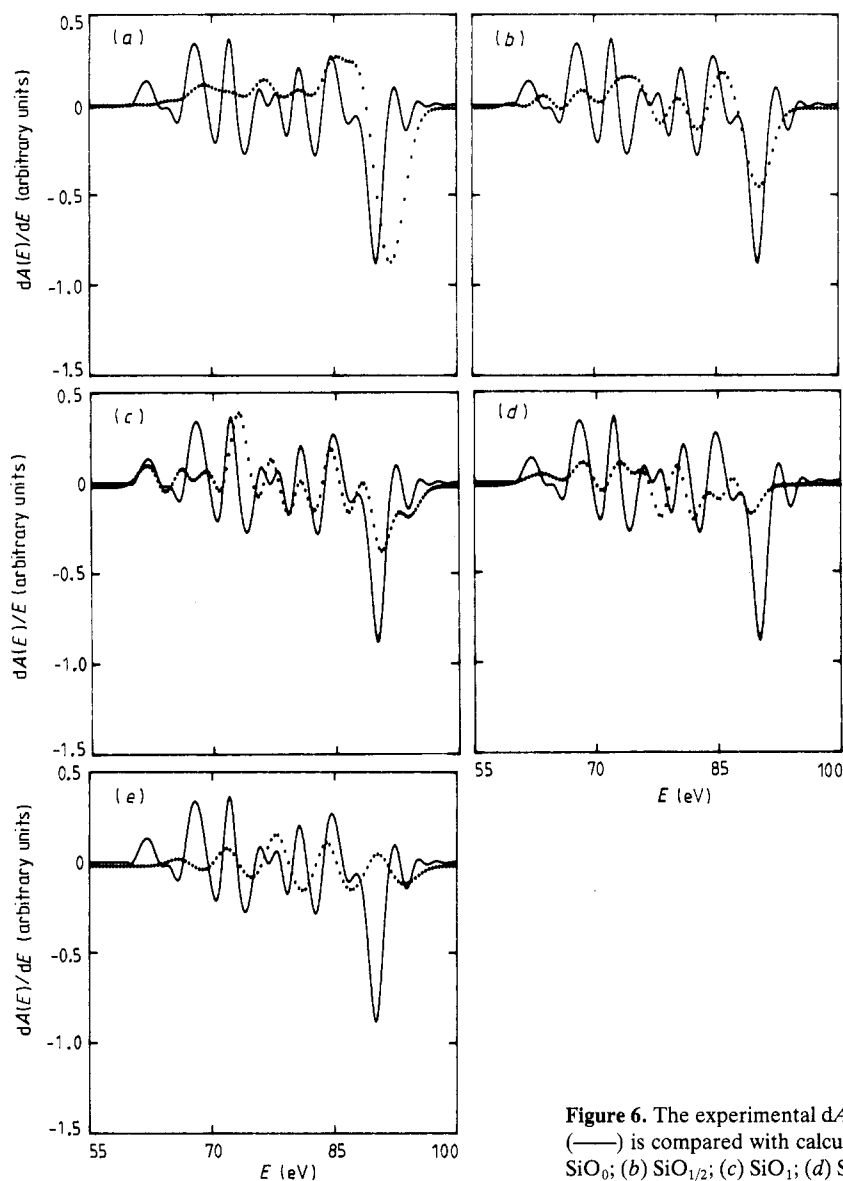
Figure 6. The experimental d$A(E)$/dE spectrum (——) is compared with calculations (······): (*a*) SiO$_0$; (*b*) SiO$_{1/2}$; (*c*) SiO$_1$; (*d*) SiO$_{3/2}$; (*e*) SiO$_2$.

molecule perpendicular to the first- or second-layer dimer. Only the nitrogen atom has been coordinated to the surface. The oxygen atom has no electronic overlap with the silicon surface. The saturation coverage is about 15% of a monolayer and therefore features related to elemental silicon will be dominant in the Auger lineshape of Si–NO.

Although the main attention is directed towards NO adsorption at 300 K, we shall present some additional experimental results performed at higher temperatures (550 and 1050 K) to force the NO molecule to dissociate [26] and to desorb from the silicon surface as SiO. The results are depicted in figure 7.

In figure 7 we present three loss-corrected experimental Auger lineshapes. The coverages related to the three curves in figure 7 are (7 + 1)% O and (7 + 1)% N
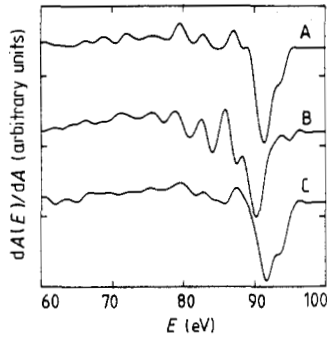
Figure 7. Experimentally obtained $dA(E)/dE$ spectra: curve A, Si(100) exposed to 2.0×10^3 L NO at 300 K; curve B, Si(100) exposed to 2.0×10^3 L NO at 550 K; curve C, Si(100) surface heated to 1050 K after finishing the exposure.
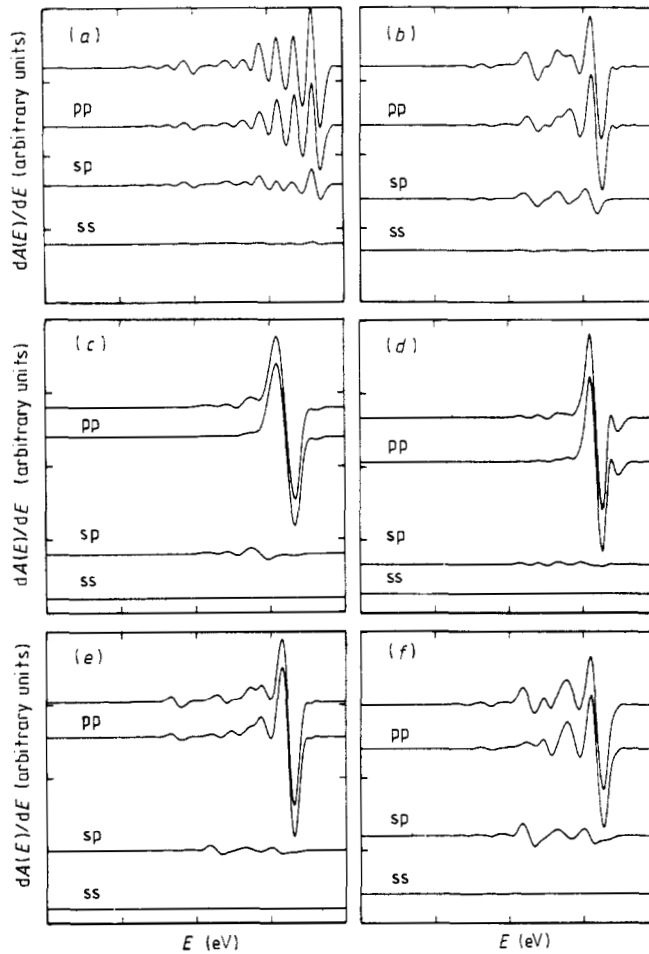
Figure 8. The calculated Auger lineshapes $(dA(E)/dE$, of Si–NO for (a)–(d) the first-layer dimer $((a)$ up atom; (b) down atom; (c) back bond connected to the up atom; (d) back bond connected to the down atom) and (e), (f) the second-layer dimer. The width of the kinetic-energy axis is 60 eV. The zero of this axis depends on the energy of the core hole and the effective values for the work functions of the surface and the detector.

for curve A, $(7 + 1)\%$ O and $(12 + 1)\%$ N for curve B and 0% O and $(12 + 1)\%$ N for curve C (per monolayer) [26]. The experimental details are listed in the figure caption of figure 7.

Significant structure in the region above the main peak for clean silicon (91.8 eV) can be observed in both the calculated and the loss-corrected experimental data. Furthermore, these features can be assigned to the dimer-up atom as the most dominant contributor (see figure 7).

The peaks at approximately 88 eV (curves A and B in figure 7) can be entirely attributed to adsorption of oxygen to the silicon surface. This is in agreement with the results in [31], where a feature at about 87 eV was observed. The shift of 1 eV could be caused by changes in the bonding configuration from predominantly molecular adsorbed oxygen to atomic oxygen.

The existence of Si–O bonds in figure 7, curve A, in which only molecular adsorption of the NO molecule was proposed could be explained if there exists an additional defect adsorption mechanism (step edges) which induces the dissociation of the NO molecule and gives rise to a small contamination of the Auger spectrum with contributions from Si–O bonds [26].

Of particular interest is the question whether we can distinguish the contribution from the NO molecule adsorbed on the first- or second-layer dimer in the experimental Auger lineshape. However, the correlation between the calculated spectra (figure 8) makes it impossible to draw definite conclusions about a predominant adsorption site.

5. Concluding remarks

In conclusion, the described approach to analyse Auger lineshapes corrected for all kinds of loss mechanism and combined with quantum chemical cluster calculations is shown to be a powerful tool for identifying Auger lineshapes in terms of the LDOS of the valence electrons. Furthermore, by analysing the Auger lineshapes in the derivative mode, subtle changes due to chemisorption of oxygen or nitrogen could be resolved and characterised.

References

[1] Holloway P H 1980 *Adv. Electron. Electron Phys.* **54** 241
[2] Ramaker D E 1982 *Springer Series in Chemical Physics* vol 20, ed. R Vanselow and R Howe (Berlin: Springer) p 19
  Ramaker D E, Hutson F L, Turner N H and Mei W N 1986 *Phys. Rev.* B **33** 2574
[3] Feibelman P J, McGuire E J and Pandey K C 1977 *Phys. Rev.* B **5** 2202
  Feibelman P J and McGuire E J 1978 *Phys. Rev.* B **17** 690
[4] Ramaker D E, Murday J S, Turner N H, Moore C, Lagally M G and Houston J E 1979 *Phys. Rev.* B **19** 5375
[5] Lander J J 1953 *Phys. Rev.* **91** 1382
[6] Hagstrum H D and Becker G E 1971 *Phys. Rev.* B **4** 4187
[7] Hagstrum H D and Becker G E 1973 *Phys. Rev.* B **8** 1580
[8] Amelio G F 1970 *Surf. Sci.* **22** 301
[9] Houston J E 1974 *J. Vac. Sci. Technol.* **12** 255
[10] Weissmann R and Muller K 1981 *Surf. Sci. Rep.* **1** 251
[11] Brockman R H and Russel G J 1980 *Phys. Rev.* B **22** 6302
[12] Sasse A G B M, Lakerveld D G and van Silfhout A 1988 *J. Vac. Sci. Technol.* A **6** 1045
[13] Ramaker D E 1985 *Appl. Surf. Sci.* **21** 243
[14] Mularie W M and Peria W T 1971 *Surf. Sci.* **26** 125

[15] Sasse A G B M, Wormeester H and van Silfhourt A 1988 *Surf. Interface Anal.* **13** 228
[16] Madden H H and Houston J E 1976 *J. Vac. Sci. Technol.* **47** 3071
[17] Madden H H and Houston J E 1977 *Solid State Commun.* **21** 1081
[18] Madden H H and Houston J E 1977 *J. Vac. Sci. Technol.* **14** 412
[19] Houston J E, Moore G and Lagally M G 1977 *Solid State Commun.* **21** 879
[20] Jennison D R 1978 *Phys. Rev.* B **18** 6865
[21] Jennison D R 1978 *Phys. Rev. Lett.* **40** 807
[22] Ramaker D E 1982 *Phys. Rev.* B **25** 7341
[23] Ramaker D E 1980 *Phys. Rev.* B **21** 4608
[24] Matthew J A D and Komninos Y 1975 *Surf. Sci.* **53** 716
[25] Keim E G, Wolterbeek L and van Silfhout A 1987 *Surf. Sci.* **180** 565
    Grunthaner F J and Grunthaner P J 1986 *Mater. Sci. Rep.* **1** 2–3
[26] Sasse A G B M and van Silfhout A 1989 *Phys. Rev.* B **40** 1773
    Sasse A G B M, Kleinherenbrink P M and van Silfhout A 1988 *Surf. Sci.* **199** 243
[27] Sasse A G B M, Wormeester H, van der Hoef M A and van Silfhout A 1989 *Surf. Sci.* **210** 553–68
[28] Wormeester H, Sasse A G B M and van Silfhout A 1988 *Phys. Comput. Commun.* **52** 19
[29] Fletcher R 1971 *UK Atomic Energy Authority Research Group, Theoretical Physics Division, Report* AERE-R.6799
[30] Prenter P M 1975 *Splines and Variational Methods* (New York: Wiley)
[31] Sasse A G B M, Wormeester H, van der Hoef M A, Keim E G and van Silfhout A 1989 *J. Vac. Sci. Technol.* A **7** 1623
[32] Chadi D J 1979 *Phys. Rev. Lett.* **43** 43
[33] Verwoerd W S 1980 *Surf. Sci.* **99** 581
[34] Kunjunny T and Ferry D K 1981 *Phys. Rev.* B **24** 4593
[35] Sasse A G B M, van der Hoef M A, Feil D and van Silfhout A 1988 *Proc. 19th Int. Conf. Physics of Semiconductors* ed. W Zawadki (Warsaw: Institute of Physics, Polish Academy of Sciences) p 741
[36] Sasse A G B M 1988 *Thesis* Faculty of Applied Physics, University of Twente, Enschede, The Netherlands
[37] Keim E G 1984 *Surf. Sci.* **148** L641
    Keim E G, Wolterbeek L and van Silfhout A. 1987 *Surf. Sci.* **180** 565
[38] Keim E G and van Silfhout A 1987 *Surf. Sci.* **187** L557
    Keim E G, van Silfhout A and Wolterbeek L 1988 *J. Vac. Sci. Technol.* A **6** 57
[39] Keim E G and van Silfhout A 1985 *Surf. Sci.* **152–153** 1096
    Keim E G, van Silfhout A and Wolterbeek L 1987 *J. Vac. Sci. Technol.* A **5** 1019
[40] Brockman R H and Russell G J 1980 *Phys. Rev.* B **22** 6302
[41] Knotek M L and Houston J E 1983 *J. Vac. Sci. Technol.* **1** 899
[42] Fiori C 1984 *Phys. Rev. Lett.* **52** 2077
[43] Fiori C and Devine R A B 1984 *Phys. Rev. Lett.* **52** 2081
[44] Hollinger G and Himpsel F J 1983 *Phys. Rev.* B **28** 3651